



“Gheorghe Asachi” Technical University of Iasi, Romania



---

## SOIL TEMPERATURE PROFILE INVESTIGATION UNDER ARID CLIMATE OF KUWAIT USING MECHANISTIC AND MIXED MODELS

Azel Almutairi\*, Suad Aladwani, Bedour Almutairi

Kuwait University, Environmental Technology Management Department, 13060, Safat, Kuwait

---

### Abstract

Soil temperature prediction at several depths is crucial for environmental, engineering, and management applications. In this study, two approaches, namely the mechanistic model and the mixed model, are used to estimate the soil temperature at depths from 0.05 m to 8 m and compared with measured data. The Carslaw-Jaeger equation's parameters, the average, the amplitude, and the phase lag, that suit an arid environment such as Kuwait are determined by the two techniques. Heat flux analyses of the soil are presented. The generated models are tested against the measured data with different statistical tests such as  $R^2$ , RMSE, and MAPE. Values of  $R^2$  for the mechanistic and the mixed models range from 0.9119 to 0.9315 and 0.9068 to 0.9268 respectively, for the depths from 0.05 m to 1 m.

*Key words:* climate change, energy budget, environmental simulation, root zone temperature

*Received:* May, 2020; *Revised final:* December, 2020; *Accepted:* December, 2020; *Published in final edited form:* July, 2021

---

### 1. Introduction

Spatial and temporal temperature distribution of the soil and its thermal properties have a great impact on determining physical, chemical, and biological processes on the soil. Temperature profile with respect to time and space, describes the transfer and accumulation of heat on the soil. Soil temperature is an important aspect for determining the heat exchange capacity between the air and the earth, underground building, pipes, agricultural greenhouse, and any heat carriers in the ground. Therefore, it is a crucial factor in energy consumption calculations, especially those that rely on degree-day methods.

Several parameters produce an effect on the heat flow inside the earth, which has a great thermal benefit to the earthen environment. These are solar radiation, air temperature, wind speed, season, shading, soil properties, etc. Therefore, predicting the soil temperature is a difficult task, and estimating soil temperature depends mainly on certain local climatic conditions and soil properties. Kuwait's climate is

considered to be harsh, which is a hot, dry, and desert type. However, the bottom soil has fewer temperature fluctuations and is less extreme. The temperature will change on a daily basis, and more clearly in a seasonal cycle, and therefore, estimating a soil temperature profile is a function of time and underground depth.

Literature reveals three approaches by which soil temperature can be predicted; the first one is the empirical approach, in which soil temperature can be determined statistically with the help of climatological variables, specifically air temperature. The second is the mechanistic approach, which is based on the ground surface energy balance theory that utilizes the balance of the energy types such as radiation, conduction, and convection and generating a partial differential equation along with applicable boundary conditions to be solved mainly by Fourier's technique. The third approach is accomplished by using the Fourier's approximation; however, the equation constants are determined empirically (mixed model). In literature, these constants are also known as the Carslaw-Jaeger equation's parameters. Simply, these

---

\* Author to whom all correspondence should be addressed: e-mail [azel.almutairi@ku.edu.kw](mailto:azel.almutairi@ku.edu.kw); Phone: +96524633100; Fax: +9652483 9146

parameters are the parameters of the waveform function. The main difference between the mechanistic approach and the mixed model is how to find the waveform function's parameters. In the mechanistic model, these parameters are found analytically, while in the mixed model, they are found with approximations using climatic data. The mixed model is usually known as the Labs' equation (Al-Temeemi and Harris, 2001).

Previous studies were carried out to predict the soil temperature profile for specific site in Kuwait. Due to the geographic homogeneity of Kuwait, this site might be representative. Moustafa et al. (1981) estimated a soil temperature model using the Labs' equation and climatic data only for one year. This model was compared with the soil temperature measurements and the accuracy was +/- 1.2 °C (Moustafa et al., 1981). Khatry, et al.(1978) developed an analysis of ground temperature variations for specified depths using a Fourier analysis model and with the assumption that the temperature is equal to the sol-air temperature. (Al-Temeemi and Harris, 2001) predicted subsurface temperature profiles for various depths. The model profile was based on Labs' equation for subterranean temperature and was used to analyze the seasonal variations of temperatures at various depths and duration.

Continuous and sufficient experimental measurements of temperature distribution should be performed for a long period of time. This can reflect the real temperature profile for a certain location and reduce errors. Mathematical models based on the heat balance equation on the ground surface are expected to give accurate approximations of soil temperature (Larwa, 2019; Mihalakakou et al., 1997; Mihalakakou, 2002) and were never applied to Kuwait's climatic data. The objectives of this study

are as follows: (1) examining the soil temperature data in Kuwait, (2) building the mixed model that is appropriate for Kuwait, and (3) applying the mechanistic soil temperature approach insight of the measured data and comparing the results to the mixed model.

## 2. Material and methods

### 2.1. Study area overview

Kuwait has a desert and a hot, arid climate zone, which is characterized by its long summer and short winter. During the summer, temperatures are extremely high, while during the winter the weather is dry. The average annual rainfall of this region is 0.175 m, and the mean annual maximum and minimum temperature are 45°C and 28°C in summer and 35°C and 14°C in winter. There is an average of 3,347 hours of sunlight per year. (Fig. 1) shows the location of the weather station that is under study.

### 2.2. Meteorological data

Soil temperature,  $T_s$  (°C) data from 2016 to 2019 at 0.05, 0.20, 0.50, and 1.00 m depths were obtained from the Meteorological Department of the Directorate of Civil Aviation and collected at a local weather station as shown in (Fig. 1), along with other climatological data, including air temperature, dew temperature, wind speed, humidity, and solar radiation. Long-term data (from 1963 to 2020) for air temperature was obtained from the National Climatic Data Center (NCDC, USA) for the same studied weather station (Station ID number is 40582). The monitoring site's soil is sandy, not shaded, and its color is light grey. The monitor site elevation is 46 m.

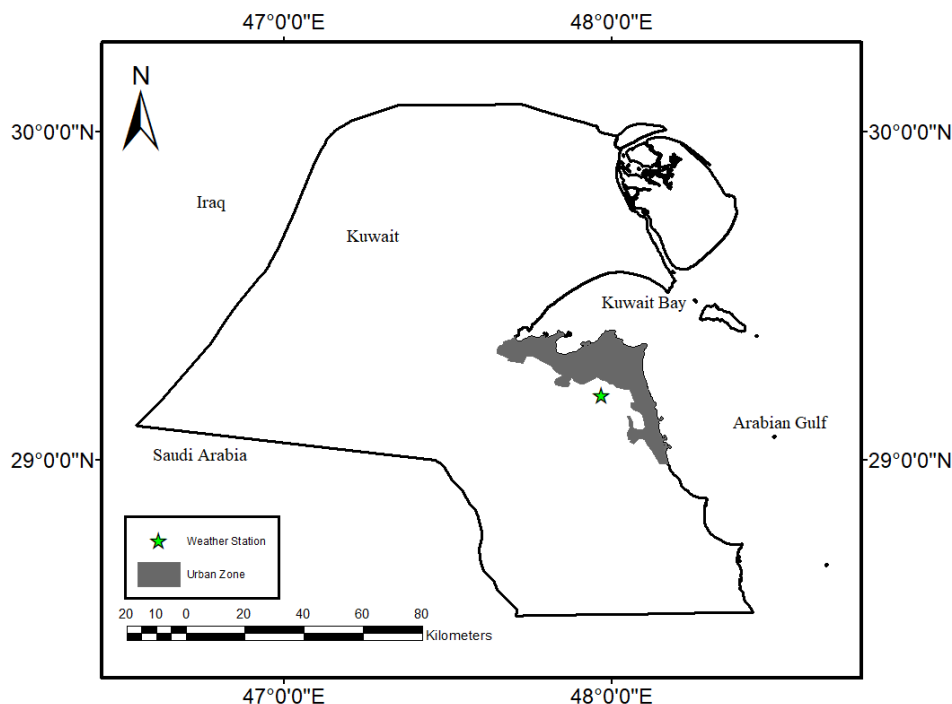


Fig. 1. Weather station under study

### 2.3. Analytical model

The undisturbed ground temperature at subsurface depth  $x$ , assuming the soil volumetric heat capacity ( $C_s$ , J/K·m<sup>3</sup>) and its thermal conductivity ( $k_s$ , W/m·K) are independent of depth, can be modeled with the Fourier law of heat conduction for a vertical one-dimensional medium (Mihalakakou et al., 1997) as given in (Eq. 1):

$$\frac{\partial^2 T_s(x,t)}{\partial x^2} = \frac{1}{\alpha_s} \frac{\partial T_s(x,t)}{\partial t} \quad (1)$$

where  $\alpha_s$  (m<sup>2</sup>/s) is the thermal diffusivity of soil and  $t$  is time in seconds (s). According to (Carslaw and Jaeger, 1986; Kusuda and Achenbach, 1965; Krarti et al., 1995) the soil temperature  $T_s(t)$  change periodically around a mean value,  $T_m$ , which is the average temperature in the soil during one year, as in (Eq. 2):

$$T_s(t) = T_m + T_v \operatorname{Re}(e^{i\omega t}) \quad (2)$$

where  $T_v$  (°C) is the amplitude of the temperature variation and  $\operatorname{Re}$  is the real part of the complex argument, and  $\omega$  is the frequency of the temperature variation. For an annual cycle,  $\omega = 2\pi / 365 \text{ day}^{-1} = 1.992 \times 10^{-7} \text{ rad/s}$ .

At the soil, to solve (Eq. 1), the first boundary condition is obtained by applying energy balance (Krarti et al., 1995) as shown in (Eq. 3) and (Fig. 2):

$$-k_s \left. \frac{\partial T_s}{\partial x} \right|_{x=0} = H + S_r - R - E_w \quad (3)$$

where the left-hand side of (Eq. 3),  $q_c$  is the conductive heat flux (W/m<sup>2</sup>),  $R$  is the long-wave radiation heat flux (W/m<sup>2</sup>),  $H$  is the convective heat flux (W/m<sup>2</sup>),  $S_r$  is the solar radiation heat flux (W/m<sup>2</sup>) that is absorbed from the ground surface, and  $E_w$  is the evaporative heat flux (W/m<sup>2</sup>). In (Eq. 3), flux sign convention was chosen so that all energy fluxes are defined as being positive when directed toward the surface.

The second convenient boundary condition (Larwa, 2019) is based on neglecting geothermal flux and hence, no variation of surface temperature at greater depth ( $x_\infty$ ) is observed as (Eq. 4) shows:

$$\text{at } x = x_\infty, \frac{dT}{dx} = 0 \quad (4)$$

In Carslaw and Jaeger (1986) a solution to Eq. (1) was provided, using the boundary conditions discussed above, by which the soil temperature can be predicted as a function of depth level and time as described in (Eq. 5):

$$T(x,t) = T_m - T_v \cdot e^{-\frac{x}{D}} \cdot \cos(\omega t - \varphi_s - \frac{x}{D}) \quad (5)$$

where  $\varphi_s$  is phase angle (rad), and  $D$  is the damping depth (m) that is defined as (Eq. 6):

$$D = \sqrt{\frac{2\alpha_s}{\omega}} \quad (6)$$

Damping length is a parameter describing the decrease in soil temperature amplitude as the ground depth level increases (Krarti et al., 1995; Larwa, 2019). For instance, at  $x = D$ , the soil temperature amplitude at the surface is  $e$  times the amplitude at that depth (Krarti et al., 1995); where  $e$  is Euler's number. The energy fluxes involved in (Eq. 3) are discussed below, and an annual soil temperature model can be developed.

#### 2.3.1. Convective heat flux, $H$

This type of heat flux is due to the heat exchanged between the soil and the air, and its magnitude entirely depends on the driving force, which is the difference between the soil temperature,  $T_s(0,t)$ , and the air temperature,  $T_a$ , and the convective heat transfer coefficient at the surface,  $h_s$ .  $H$  can be evaluated by the classical convective heat transfer Equation as in (Eq. 7):

$$H = h_s [T_a - T_s] \quad (7)$$

The convective heat transfer coefficient at the surface,  $h_s$ , mainly depends on wind speed,  $u$ , and can be estimated linearly from (Mcadams, 1954) as stated in (Eq. 8):

$$h_s = 5.7 + 3.8u \quad (8)$$

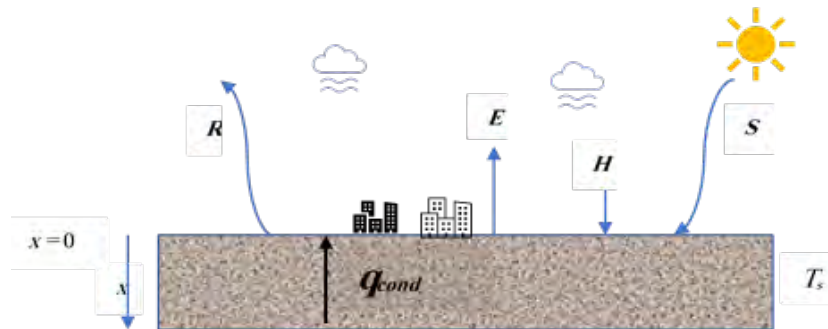


Fig. 2. Energy balance on the surface of the ground

The daily air temperature,  $T_a$ , can be approximated as a harmonic function as shown in (Eq. 9):

$$T_a = T_{ma} - T_{va} \cos(\omega t - \phi_a) \tag{9}$$

where  $T_{ma}$  (°C) and  $T_{va}$  (°C) are the averages and the amplitude of the air temperature wave at  $2\pi/\omega$ , respectively, and  $\phi_a$  (rad) is the phase angle.

2.3.2. Shortwave radiation heat flux,  $S_r$

Solar radiation is the incoming,  $S_0$ , and outgoing radiation in the shortwave band (Shuttleworth, 2012). According to solar radiation analysis, the absorbed shortwave radiation heat flux can be evaluated (Kreith et al., 2010) from (Eq. 10):

$$S_r = \beta S_0 \tag{10}$$

where  $\beta$  is the absorption coefficient that depends on the soil absorption and shading, and it can be estimated to one minus the surface albedo (Krarti et al., 1995). For bare soil, dry clay,  $\beta$  can be taken as 0.8 (Shuttleworth, 2012). Shortwave solar radiation can be approximated by the following waveform as (Eq. 11) stated (Mihalakakou et al., 1997):

$$S_r = \beta[S_m - S_v \cos(\omega t - \phi_1)] \tag{11}$$

where  $S_m$  (W/m<sup>2</sup>) and  $S_v$  (W/m<sup>2</sup>) are the averages and the amplitude of the shortwave solar radiation sinusoidal function, respectively, and  $\phi_1$  (rad) is the phase angle.

2.3.3. Longwave radiation heat flux,  $R$

The longwave ground radiation conforms to the Stefan–Boltzman Law (Shuttleworth, 2012) and it can be considered approximately constant (Mihalakakou et al., 1997) with the following formula as shown in (Eq. 12) (Krarti et al., 1995):

$$R = \varepsilon \Delta R \tag{12}$$

where  $\varepsilon$  is emittance of the ground surface and can be calculated from various empirical correlations that mainly depend on dew temperature,  $T_{dew}$ , as elaborated in (Walton, 1983).  $\Delta R$  is a parameter that depends on several variables among which are relative humidity,  $r$ , sky temperature,  $T_{sky}$ , and the air above the ground surface. For a horizontal surface, a value of 63 W/m<sup>2</sup> is reasonable for  $\Delta R$  (Khatri et al., 1978).

2.3.4. Evaporative heat flux,  $E_w$

Evaporation is a complex phenomenon, and consequently, the estimation of energy due to evaporation is a complicated task (Almutairi, 2019). However, several authors utilized meteorological parameters to develop models to estimate the evaporation rate from the soil. Penman in 1948 (Penman, 1948) provided a model to evaluate evaporative heat flux from bare soil as given by Eq. (13):

$$E_w = 0.0168 fh_s [(103T_s + 609) - (103T_a + 609)] \tag{13}$$

where  $f$  is the fraction of the potential evaporation rate and it depends on the soil cover and the soil moisture level, and it ranges from 0.1 to 0.2 for arid soils (Krarti et al., 1995).

2.3.5. Determination of  $T_m$ ,  $T_v$ , and  $\phi_s$

$T_m$ ,  $T_v$ , and  $\phi_s$  are the parameters that are required to determine the soil temperature profile distribution. To find  $T_m$ , the yearly average conductive heat flux is set to equal zero (Gwadera et al., 2017; Khatri et al., 1978; Krarti et al., 1995; Mihalakakou et al., 1997), and by substituting all energy flux expressions in (Eq. 3), and substituting (Eq. 9) and (Eq. 11) in (Eq. 7), the following expression will be obtained which defines  $T_m$  (Eq. 14):

$$T_m = \frac{1}{h_s(1 + 0.0168af)} [(h_s(1 + 0.0168arf))T_{ma} - \varepsilon \Delta R + \beta S_m - 0.0168h_s fb(1 - r)] \tag{14}$$

where  $a = 103$  Pa/K and  $b = 609$  Pa are the saturated vapor pressure constants. To find  $T_v$ , the first derivative of Eq. (2) with respect to  $x$  must be performed and used in (Eq. 3). The result is shown in Eq. (15).

$$T_v = \left\| \frac{h_r T_{va} - \beta S_v e^{i\omega t}}{h_e + \delta k_s} \right\| \tag{15}$$

and consequently (Eq. 16),

$$\phi = -Arg \left[ \frac{h_r T_{va} - \beta S_v e^{i\omega t}}{h_e + \delta k_s} \right] \tag{16}$$

where the  $\| \quad \|$  and  $Arg$  are, respectively, the modulus and the argument of a complex number.  $\Delta$  is defined as (Eq. 17):

$$\delta = \sqrt{\frac{i\omega}{a_s}} = \frac{1+i}{D} \tag{17}$$

2.4. Mixed model (Labs' equation)

The Labs' equation (Labs, 1979) for estimating the subsurface temperature as a function of time and depth is similar to Eq. (5) and it has the following form (Eq. 18):

$$T(x, t) = T_m - T_v \cdot e^{-x\sqrt{\pi/365a_s}} \cdot x \cos \left\{ \frac{2\pi}{365} \left[ t - t_0 - \left( \frac{x}{2} \right) \right] \right\} \tag{18}$$

where  $t_0$  is the Labs' equation phase constant which corresponds to the day of minimum surface

temperature. According to (Watson and Labs, 1993),  $T_m$  can be approximated as in (Eq. 19):

$$T_m(^{\circ}C) = 1.7 + \bar{T}_{a,long} (^{\circ}C) \quad (19)$$

where  $\bar{T}_{a,long}$  is the long-term average annual air temperature. For this study, the average long-term air temperature (1963-2020) is 26.56 °C, thus,  $T_m$  will be 28.26 °C.  $T_v$  can be estimated from the suggestion of (Watson and Labs, 1992) as shown in Eq. (20):

$$T_v(^{\circ}C) = 1.1 + \frac{1}{2} [\bar{T}_{a,July} - \bar{T}_{a,January}] \quad (20)$$

where  $\bar{T}_{a,July}$  and  $\bar{T}_{a,January}$  are the July and January monthly average air temperature, respectively in °C. Using data obtained from NCDC, the long-term (1963-2020) July and January monthly average air temperatures are 38.68 and 13.00°C, respectively, thus,  $T_v$  will be 13.94. The Labs' equation phase constant,  $t_0$ , refers to the Julian  $n^{\text{th}}$  day of minimum surface temperature (Al-Temeemi and Harris, 2001). Since this information is not available, instead, the phase of a solar radiation wave can be used as an indicator for the wave of surface temperature, as the former lags behind the latter by 1/8 of the cycle or approximately 46 days (Al-Temeemi and Harris, 2001). In this study, it was found that the lowest solar energy occurred on day 343 of the year, thus,  $t_0$  takes a value of 24. (Table 1) shows a comparison of Labs' equation parameters of studies done on Kuwait's soil.

**Table 1.** Labs' equation parameters of studies done on the Kuwait soil

Reference	$T_m$ (°C)	$T_v$ (°C)	$t_0$
Al-Temeemi and Harris (2001)	27.30	13.6	36
Moustafa et al. (1981)	27.78	10.56	26
This Study	28.26	13.94	24

### 2.5. Model testing

To test how a model performs, there are a few quantitative measures used in the literature for this purpose, such as the coefficient of determination  $R^2$ , root mean square error (RMSE) and mean absolute percentage error (MAPE, %).  $R^2$  describes the variability explained by the model and it ranges from 0 to 1. The higher the  $R^2$  value the better the model is. RMSE is a statistical error test that should be close to zero for a good performance and it has the following form (Eq. 21):

$$RSME = \sqrt{\frac{1}{n} \sum_{i=1}^n [F_i - a_i]^2} \quad (21)$$

where  $F_i$  is the predicted value,  $A_i$  is the measured data, and  $n$  is the number of data points. MAPE is a percentage error and it is expressed as given by Eq. (22):

$$MAPE = \frac{1}{n} \sum_{i=1}^n \left| \frac{F_i - A_i}{A_i} \right| \times 100 \quad (22)$$

The smaller the MAPE values, the closer are the predicted data to the measured ones. (Lewis et al. 1983) classified model's performance with its obtained MAPE values and the literature categorized models with MAPE of 10 % or less as "very good" in predicting the measured values, those with 10 to 20 % as "good", 20 to 50 % as "acceptable", and 50 % or over are "wrong and faulty."

## 3. Results and discussion

### 3.1. Data investigation

The observation of soil temperature for the years 2016 to 2019 at different depths are depicted and compared to the daily average air temperature in Fig. 3. According to Fig. 3, the fluctuations and the values of soil temperature at depths of 0.05 m and 0.20 m for the mentioned years are similar and have close values. By examining the results of (Mihalakakou et al., 1997), it is found that the soil temperature at a depth of 0.30 m fluctuates critically over time. This observation is also true for the work done by (Sharma et al., 2010). Fig. 3 also reveals that the waveform curve at the depth of 0.50 m, and more clearly at the depth of 1.00 m are smoother and have less fluctuation than the 0.05 m and the 0.20 m graphs.

It is also observed that the first and the last 50 days of the graphs in (Fig. 3), the 1.00 m depth graph has the highest soil temperature values when compared to the soil temperature values at other depths. However, the 1 m depth is the lowest from approximately 50 to 260 days. The same pattern is depicted by (Moustafa et al., 1981) for depths equal to 3.60 m in the first 90 days as the maximum soil temperature of a range of depths from 0.60 m to 3.60 m. The mean soil temperature at depths 0.05 m, 0.20 m, 0.50 m, and 1.00 m are 31.00°C, 30.89, 30.52°C, 30.20°C respectively.

### 3.2. Model's performance

A comparison between the predicted data using the developed models and the measured data for a depth of 0.05 m and the years from 2016 to 2019 is shown in Fig. 4. For the Analytical model, the values of  $T_m$ ,  $T_v$ , and  $\phi_s$  found by Eqs. (14-16) are 25.58°C, 12.11°C, and 0.40 rad, respectively. The Labs parameters serving to characterize the waveform function were presented in (Table 1). All regressions in Fig. 4 are statistically tested with an analysis of variance (ANOVA) and they were found statistically significant with a p-value of less than 0.0001. (Fig. 4a) shows how precise the analytical model represented the measurement results. Fig. 5 shows the consistency of the Analytical model with the measured data using 5% of the significance level.

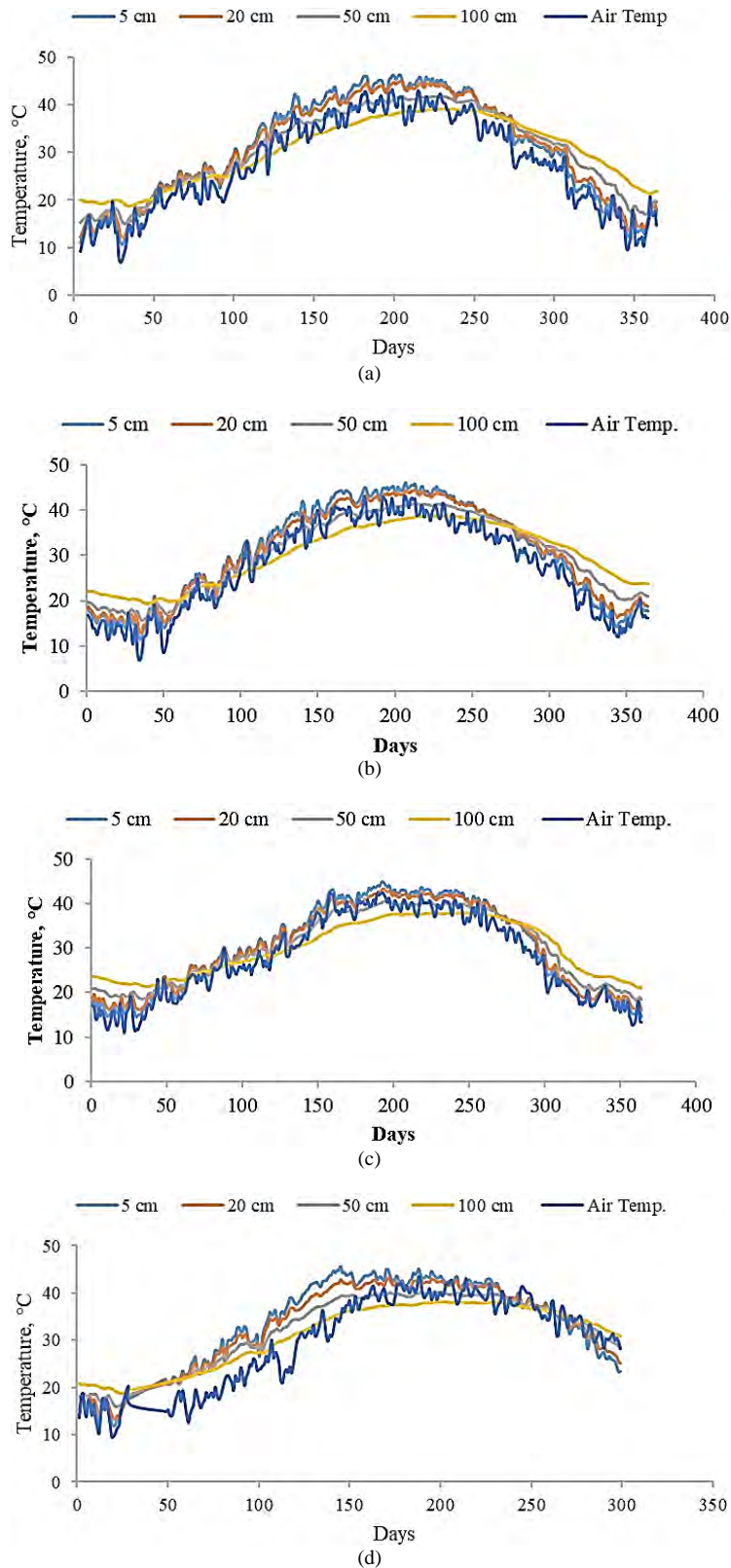


Fig. 3. Soil temperature at various depths and average daily air temperature: (a) 2016, (b) 2017, (c) 2018, and (d) 2019

The performance of each model is evaluated by the statistical tests discussed in section 2.5 and documented in (Table 2). It can be observed from (Table 2) that all statistical tests, for all models, improve as the depth increases, thus, the models performed better. This may refer to the fluctuations,

discussed above, associated with decreased depths. Also, the Analytical model performed better than any other model at all depths with  $R^2$  ranged from 0.9119 to 0.9315 increasing with depth. Indeed, the Analytical model had an advantage over the other models using all performance tests, except Moustafa's

model, which has slightly higher values of *RSME* and *MAPE* compared to the Analytical model.  $R^2$  of Labs' equation is slightly higher than Moustafa. Thus, considering *RSME* and *MAPE*, Moustafa's model performed better than the Labs' equation model. Al-Tameemi's model ranks last with all used tests. Except for the Labs' equation model, all models have *MAPE* values of less than 10 %.

The Labs' Equation model had the highest *MAPE* value of 15.51 % for 0.05 m. While the Labs' equation model categorized as "very good" for 1.00 m, it classified as "good" for the other depths. *RMSE* values reported by (Kemp et al., 1992) for depth 0.01 m, 0.01 m, and 0.20 m were 3.99 °C, 2.39 °C, and 1.59 °C, respectively, which are higher than the Analytical model's *RMSE* values.

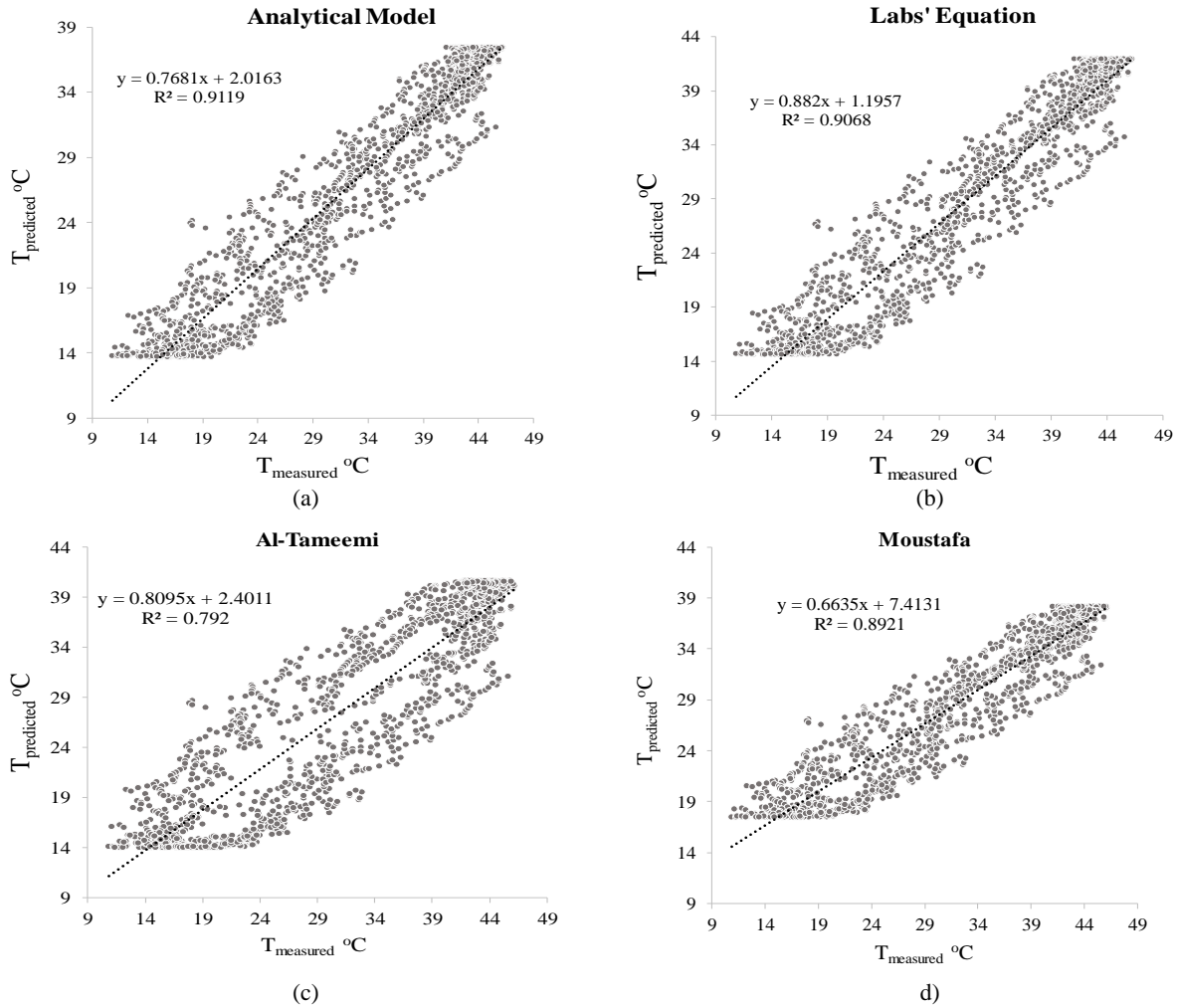


Fig. 4. Predicted values in plotted against the measured data using: (a) Analytical model, (b) Labs' equation, (c) Al-Tameemi's Model, and (d) Moustafa's Model

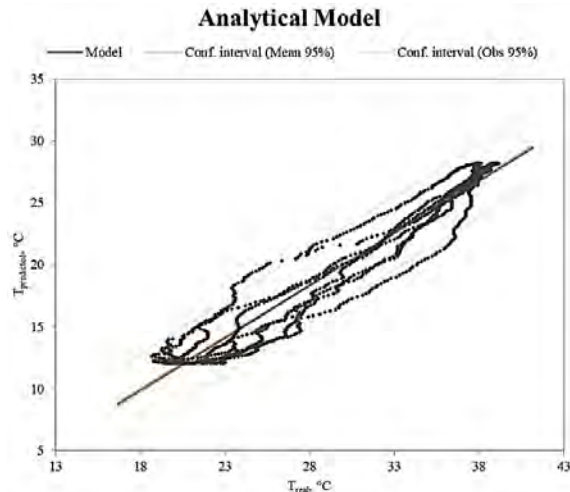


Fig. 5. The consistency of the Analytical model with the measurement values

**Table 2.** Model’s statistic analysis

Test	Analytical	Labs	Al-Tameemi	Moustaafa
0.05 m				
R <sup>2</sup>	0.9119	0.9068	0.7920	0.8921
RMSE (°C)	2.49	2.95	4.33	2.41
MAPE	8.88	15.51	9.67	7.65
0.20 m				
R <sup>2</sup>	0.9190	0.9140	0.7993	0.8994
RMSE (°C)	2.26	2.68	4.02	2.20
MAPE	7.99	14.29	8.70	6.97
0.50 m				
R <sup>2</sup>	0.9246	0.9196	0.8059	0.9052
RMSE (°C)	1.94	2.31	3.51	1.90
MAPE	6.84	12.39	7.45	6.05
1.00 m				
R <sup>2</sup>	0.9315	0.9268	0.8154	0.9127
RMSE (°C)	1.52	1.81	2.81	1.50
MAPE	5.19	9.66	5.66	4.69

Considering environmental and energy conservation, and hence, the natural resources consumption, finding alternative effective energy generation is crucial. A simple and reliable technique in determining the effectiveness of energy efficiency measures is the degree-days technique of cooling and heating (Lhag and Ahrawi, 2019). The cooling degree-days method is functioned on the assumption that power consumption is proportional to the difference between the daily mean temperature and cooling the base temperature. The difference in cooling degree-days of the above and subsurface with a base of 25.5 °C compared to the results of (Al-Temeemi and Harris, 2001) was documented in (Table 3). The accumulated cooling degree-days are computed using Eq. (23):

$$CDD = \sum_{j=1}^N (CDD_j) \begin{cases} IF, T_{md} > T_b, then CDD_j = T_{md} - T_b \\ else CDD_j = 0 \end{cases} \quad (23)$$

where  $T_{md}$  and  $T_b$  are the daily mean air temperature and the base temperature respectively.

The values in the parentheses in (Table 3) indicate the % reduction from the previous depth. In their CDD calculations, (Al-Temeemi and Harris, 2001) used subsurface soil temperatures predicted from their model and they started from depth 1 m to 8 m. CDD of this study is higher than of (Al-Temeemi and Harris, 2001) for aboveground and 1 m depth, while it is lower for the remaining depths. As (Table 3) shows, CDD decreases with increasing depth, and thus, the less demand is required for energy needed to cool earth-sheltered buildings. The drastic percentage reduction is deducted at a depth of 2 m for both this study and (Al-Temeemi and Harris, 2001). Starting at a depth of 5 m, for (Al-Temeemi and Harris, 2001), CDD stabilized at a value of 657. For this work, the percentage reduction in CDD for the depths ranging from 3 m to 8 m had a mean value of 30.6 and a standard deviation of 1.6. CDD values are calculated based on soil temperatures that were obtained from the Analytical model, excluding the measured range, with  $T_m = 25.58$  °C,  $T_v = 12.11$  °C, and  $\phi_s = 0.4$  rad.

**Table 3.** A comparison of above and subsurface cooling-degree days for 2016

Depth	Cooling Degree-Days, CDD*	Cooling Degree-Days, CDD**
Aboveground	1924	1540
Subsurface, m		
0.05	2782	-
0.20	2652 (4.7)	-
0.50	2365 (10.8)	-
1.00	2049 (13.3)	1409
2.00	647 (68.4)	1070 (24.1)
3.00	438 (32.2)	851 (20.5)
4.00	298 (32.1)	719 (15.5)
5.00	204 (31.5)	657 (8.6)
6.00	141 (30.6)	657 (0.0)
7.00	100 (29.4)	657 (0.0)
8.00	72 (27.7)	657 (0.0)

\* This work; \*\* Al-Temeemi and Harris (2001)

The temperature-depth profiles in the ground for January, April, July, and October (from 2016 to 2019) are presented in (Fig. 6) which are the monthly mean data. The data used in (Fig. 6) are two types, first, the range from 0.05 m to 1 m is the measured data and second, the range that is greater than 1 m is generated by the Analytical model.

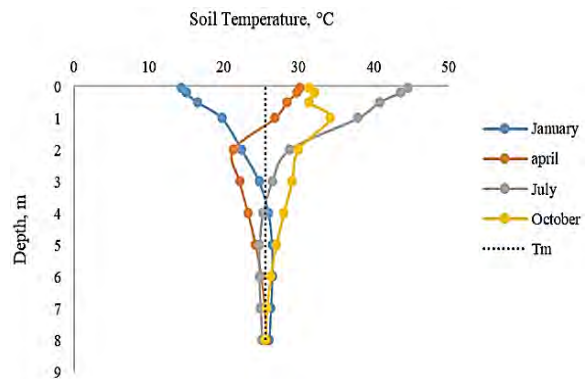


**Fig. 6.** Soil temperature distribution in subsurface depth

The dashed line represents  $T_m$ , the average

temperature in the soil. At increased depths, starting from  $x = 5$  m, all months' soil temperatures are aligned and stabilized around  $T_m$  (25.58°C). This pattern is observed in many studies such as (Labs, 1979; Larwa, 2019). However, this finding supported the second boundary condition that was used to solve (Eq. 1). It is worthy to mention that the standard deviation of soil temperature for 0.05 m, 0.20 m, 0.50 m, and 1.00 m of the months January, April, July, and October are 2.43, 1.52, 3.00, and 1.35 respectively.

### 3.3. Analysis of heat fluxes on the ground

The dependence of the Analytical model on the evaporation fraction is shown in (Fig. 7). It is proven by (Fig. 7) that as the evaporation fraction increases, the soil mean temperature and the soil amplitude decrease.

This fact emphasizes the evaporative cooling phenomenon, by which, liquid water molecules absorb heat during its conversion to vapor water, and that leads to a drop in temperature in the vicinity of these molecules including the soil itself. This behaviour was also observed by Krarti et al. (1995) and Mihalakakou et al. (1997).

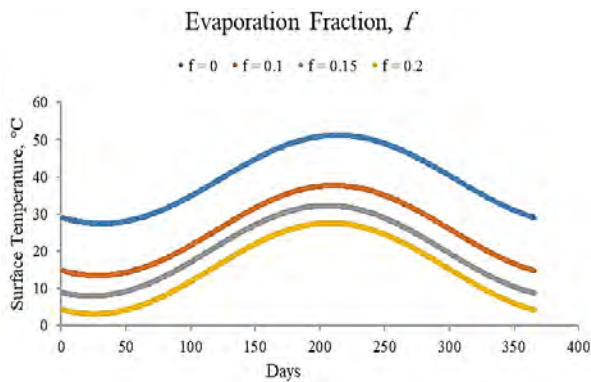


**Fig. 7.** Soil temperature's temporal variables with several evaporation fraction values

The dependence of soil temperature, predicted by the Analytical model, is shown in Fig. 8. Fig. 8a shows the entire period of soil temperature and the box on it is enlarged and expressed in Fig. 8b. As shown in Fig. 8a-b, as the relative humidity increases, the soil temperature increases as well. This finding confirms that an increment in relative humidity results in slowing the evaporation rate, and consequently, an increase in soil temperature.

The conductive heat flux variation for the year 2016 is shown in (Fig. 8c). The conductive heat flux can be estimated by differentiating (Eq. 2) with respect to  $x$  and multiply the result by the thermal conductivity as given in Eq. (24):

$$-k_s \left. \frac{\partial T_s(x,t)}{\partial x} \right|_{x=0} = \frac{k_s}{D} T_v [\cos \omega t - \sin \omega t] \quad (24)$$

The conductive heat flux variation is a response of all heat fluxes that are governed by (Eq. 3), as it is

a sum of the other heat fluxes. As (Fig. 8c) suggests, the conductive heat flux is transported from the surface into subsurface ground layers during the spring and summer; while it transfers from subsurface levels towards the surface during the autumn and winter. In (Fig. 8c), the area under the sinusoidal curve below the time axis is equal to the area above it, hence, they are canceling out each other and proving that the yearly average value of the conductive heat flux is zero.

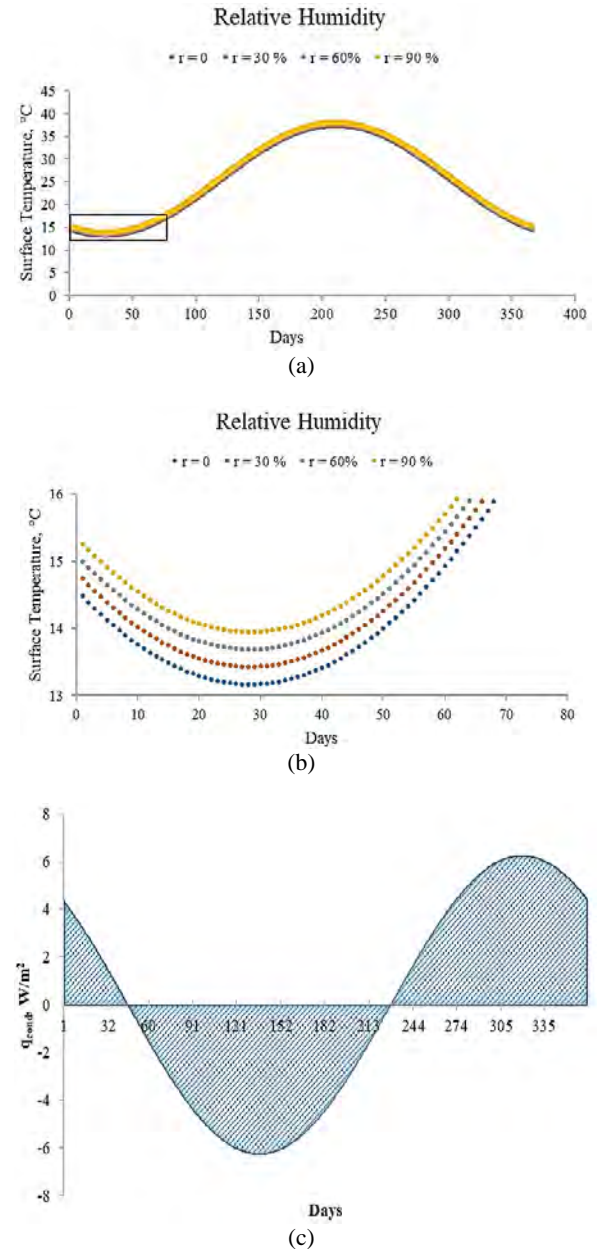


**Fig. 8.** Effect of relative humidity on soil surface temperature and the temporal conductive heat flux; (a) the entire period of relative humidity effect, (b) specific range of (a), and (c) conductive heat flux temporal variation

## 4. Conclusions

In this study, predicting the temporal variation of soil temperature at different depths was achieved by

applying two approaches, namely the mechanistic approach and the mixed model approach.

The mechanistic approach was conducted by solving the heat energy balance at the surface and determining the waveform function's constants analytically, while the same parameters were determined in the mixed model approach with the aid of the measured data. Also, the mixed model's studies, two studies, that previously performed in Kuwait was revisited for comparison and further analysis. It was found that the analytical model has a good match with the measured data, while the Labs' equation performance entirely depends on the quality of the meteorological data used.

## References

- Al-Temeemi A.A., Harris, D.J., (2001), The generation of subsurface temperature profiles for Kuwait, *Energy and Buildings*, **33**, 837-841.
- Almutairi A., (2019), Evaporation estimation of a temporary pond in arid region using aerodynamic, combined, and energy balance models, *International Journal of Engineering Research and Technology*, **12**, 1769-1777.
- Carlsaw H.S., Jaeger J.J.C., (1986), *Conduction of Heat in Solids*, 2nd Edition, Clarendo Press.
- Gwadera M., Larwa B., Kupiec K., (2017), Undisturbed ground temperature-Different methods of determination, *Sustainability*, **9**, <http://doi.org/10.3390/su9112055>.
- Khatry A.K., Sodha M.S., Malik M.A.S., (1978), Periodic variation of ground temperature with depth, *Solar Energy*, **20**, 425-427.
- Krarti M., Lopex-Alonzo C., Claridge D.E., Kreider J.F., (1995), Analytical model to predict annual soil surface temperature variation, *Journal of Solar Energy Engineering*, **117**, 91-99.
- Kreith F., Manglik R.M., Bohn M., (2010), *Principles of Heat Transfer*, 7th Edition, Stanford: Cengage Learning, Inc., United States of America.
- Kusuda T., Achenbach P.R., (1965), Earth Temperature and Thermal Diffusivity at Selected Stations in United States, ASHRAE Transactions, 71(Part 1), On line at: <https://nvlpubs.nist.gov/nistpubs/Legacy/RPT/nbsrepor t8972.pdf>.
- Labs K., (1979), Underground building climate, *Solar Age*, **4**, 44-50.
- Larwa B., (2019), Heat transfer model to predict temperature distribution in the ground, *Energies*, **12**, <http://doi.org/10.3390/en12010025>.
- Lewis C.D., Borough Green, Sevenoaks K., (1983), Industrial and business forecasting methods, *Journal of Forecasting*, Wiley, **2**, 144, <http://doi.org/10.1002/for.3980020210>.
- Lhag E., Ahrawi M.B., (2019), Economic Evaluation of a Passive Solar Greenhouse Heating System in Crete, Greece, *Applied Ecology and Environmental Research*, **17**, 4431-4446.
- Mcadams W., (1954), *Heat Transmission*, 3rd Edition, McGraw-Hill, New York.
- Mihalakakou G., Santamouris M., Lewis J.O., Asimakopoulos D.N., (1997), On the application of the energy balance equation to predict ground temperature profiles, *Solar Energy*, **60**, 181-190.
- Mihalakakou G., (2002), On estimating soil surface temperature profiles, *Energy and Buildings*, **34**, 251-259.
- Moustafa S., Jarrar D., el-Mansy H., Al-Shami H., Brusewitz G., (1981), Arid soil temperature model, *Solar Energy*, **2**, 83-88.
- Sharma P., Shukla M.K., Sammis T.W., (2010), Predicting soil temperature using air temperature and soil, crop, and meteorological parameters for three specialty crops in Southern New Mexico, *Applied Engineering in Agriculture*, **26**, 47-58.
- Penman H.L., (1948), Natural evaporation from open water, bare soil and grass, *Proceedings of the Royal Society of London. Series A, Mathematical and Physical Sciences*, **139**, 120-145.
- Shuttleworth W.J., (2012), *Terrestrial Hydrometeorology*, John Wiley & Sons, Ltd., Chichester, UK.
- Walton G., (1983), *Thermal Analysis Research Program Reference Manual*, USA, On line at: <https://www.govinfo.gov/content/pkg/GOVPUB-C13-6176908b08a357a0ac91a8ab3db55b97/pdf/GOVPUB-C13-6176908b08a357a0ac91a8ab3db55b97.pdf>.
- Watson D., Labs K., (1993), *Climatic Building Design: Energy-Efficient Building Principles and Practices Paperback*, McGraw-Hill.